

nffa.eu

PILOT 2021 2026

DELIVERABLE REPORT

WP14 JA4 - A safe-by-design platform for nanomaterials

D14.5

Production and report of three case studies with selected workflows

Due date

M51



This initiative has received funding from the EU's H2020 framework program for research and innovation under grant agreement n. 101007417, NFFA-Europe Pilot Project

PROJECT DETAILS

PROJECT ACRONYM

NEP

PROJECT TITLE

Nanoscience Foundries and Fine Analysis - Europe|PILOT

GRANT AGREEMENT NO:

101007417

FUNDING SCHEME

RIA - Research and Innovation action

START DATE

01/03/2021

WORK PACKAGE DETAILS

WORK PACKAGE ID

WP14

WORK PACKAGE TITLE

JA4 A safe-by-design platform for nanomaterials

WORK PACKAGE LEADER

Dr. Hiram Castillo (ESRF)

DELIVERABLE DETAILS

DELIVERABLE ID

D14.5

DELIVERABLE TITLE

Production and report of three case studies with selected workflows

DELIVERABLE DESCRIPTION

Preliminary results of three case studies evaluating the interaction and uptake of ZnO and TiO₂ nanoparticles in dermal (NIH-3T3), airways (BEAS-2B), and intestinal (Caco-2) cells, integrating flow microfluidics, aerosol or immersion exposures, and correlative synchrotron μ XRF/ μ XANES and electron microscopy analyses.

DUE DATE

M51 31/05/2025

ACTUAL SUBMISSION DATE

20/06/2025

AUTHORS

J. Linell (LUND), C. Isaxson (LUND), C. Abrahamsson (LUND), Maria Enea (INL), Ernesto Alfaro-Moreno (INL), V. Vilas-Boas (INL), P. Colpo (JRC), J. Ponti (JRC), R. Ciancio (CNR), M. Brollo (CNR), J. Laishram (ASP), H.A Suarez Orduz (ESRF), H. Castillo-Michel (ESRF), E. Babaliari (FORTH), D. Xydias (FORTH), A.



Pantelaiou (FORTH), M. Kefalogianni (FORTH), S. Psilodimitrakopoulos (FORTH), P. Kavatzikidou (FORTH), A. Ranella (FORTH), E. Stratakis (FORTH), B. Sartori (TUG), A. Raddeticchio (TUG), B. Marmiroli (TUG), H. Amenitsch (TUG), M. Kefalogianni (FORTH), S. Psilodimitrakopoulos (FORTH), P. Kavatzikidou (FORTH), A. Ranella (FORTH), E. Stratakis (FORTH)

PERSON RESPONSIBLE FOR THE DELIVERABLE

Hiram Castillo-Michel (ESRF)

NATURE

- R - Report
- P – Prototype, demonstrator and case studies
- DEC - Websites, Patent filing, Press & media actions, Videos, etc
- O - Other

DISSEMINATION LEVEL

- P - Public
- PP - Restricted to other programme participants & EC: (Specify)
- RE - Restricted to a group (Specify)
- CO - Confidential, only for members of the consortium



REPORT DETAILS

ACTUAL SUBMISSION DATE

20/06/2025

NUMBER OF PAGES

24

FOR MORE INFO PLEASE CONTACT

Hiram Castillo-Michel,
Affiliation: European Synchrotron
Radiation Facility
Address: 71 Av Rue des martyrs
38000, Grenoble, France

email: castillo@esrf.fr

VERSION	DATE	AUTHOR(S)	DESCRIPTION / REASON FOR MODIFICATION	STATUS
1	15/05/2025	J. Linell (LUND), C. Isaxson (LUND), C. Abrahamsson (LUND), Maria Enea (INL), Ernesto Alfaro-Moreno (INL), V. Vilas-Boas (INL), P. Colpo (JRC), J. Ponti (JRC), R. Ciancio (CNR), M. Brollo (CNR), J. LAISHRAM (ASP), H.A SUAREZ ORDUZ (ESRF), H. Castillo-Michel (ESRF)		Draft
2	13/06/2025			Draft
3	20/06/2025	J. Linell (LUND), C. Isaxson (LUND), C. Abrahamsson (LUND), Maria Enea (INL), Ernesto Alfaro-Moreno (INL), V. Vilas-Boas (INL), P. Colpo (JRC), J. Ponti (JRC), R. Ciancio (CNR), M. Brollo (CNR), J. Laishram (ASP), H.A Suarez Orduz (ESRF), H. Castillo-Michel (ESRF), E. Babaliari (FORTH), D. Xydias (FORTH), A. Pantelaiou (FORTH), M. Kefalogianni (FORTH), S. Psilodimitrakopoulos (FORTH), P. Kavatzikidou (FORTH), A. Ranella		Final



(FORTH), E. Stratakis
(FORTH), B. Sartori (TUG),
A. Raddeticchio (TUG), B.
Marmiroli (TUG), H.
Amenitsch (TUG), M.
Kefalogianni (FORTH), S.
Psilodimitrakopoulos
(FORTH), P. Kavatzikidou
(FORTH), A. Ranella
(FORTH), E. Stratakis
(FORTH)

CONTENTS

1. Introduction	7
2 Case 1: Dynamic evaluation of ZnO nanoparticles in NIH 3T3 fibroblasts	8
2.1 Context	8
2.2 Methodology	9
2.2.1 Fabrication of PDMS substrates via soft lithography (Deliverable 14.2)	9
2.2.2 Integration of the injection system for liquids with the operando system (Deliverable 14.3)	9
2.2.3 Exposure and analysis protocols (Milestone 5 + Deliverable 14.2)	10
2.3 Results	11
2.3.1 Cell viability	11
2.3.2 Performance of the microfluidic injection system integrated with the operando system	12
2.3.3 Toxicological analysis and intracellular location of NPs	13
2.3.4 Global integration and limitations	15
2.4 Conclusions	15
3 Case 2: Aerosol exposure to TiO ₂ NPs in BEAS-2B bronchial cells	15
3.1 Context	15
3.2 Methodology	16
3.2.1 Aerosol exposure of BEAS-2B cells to TiO ₂ NPs (Milestone 29)	16
3.2.2 Sample preparation	16
3.3 Results	17
3.3.1 Preliminary results before correlative analysis (Milestone 29)	17
3.3.2 Correlative SEM/STEM and μ XRF analysis in sample 3h_TiO ₂ _24h	17
3.3.3 Validation under submerged exposure: replication of the experiment by INL	19



3.4 Conclusions	22
4 Case 3: Exposure to TiO ₂ Nps in Caco-2 colon cells	22
5 Outcomes	23
6 References	24



1. INTRODUCTION

The rapid development of engineered nanomaterials (ENMs) has created the need to establish clear and reliable methods to predict possible toxic risks before they are used in commercial products (Trump et al., 2024). This report follows the safe-by-design approach, a strategy that aims to reduce risks from the early stages of nanomaterial development. This approach suggests identifying potential toxic effects during the initial phases of design and production. To achieve this, each nanomaterial is studied in detail and then exposed to controlled conditions using cells or organisms. This helps to better understand how the physicochemical properties of the nanomaterial (such as size, shape, surface charge, or solubility) may affect its biological behavior. In this way, undesired effects can be avoided before the material is used in real products (Trump et al., 2024).

The NFFA experimental platform allows the application of this approach by combining several tools: (i) physicochemical analysis of the material, (ii) *in vitro* tests with cells, (iii) live cell imaging with microscopy, and (iv) detailed analysis after fixing the samples. In addition, advanced characterization techniques such as synchrotron radiation and transmission electron microscopy are applied, enabling high-precision study of the structure, composition, and location of the nanomaterial inside cells. Workflows of this type have also been reported in other scenarios (De Angelis et al., 2025).

In this context, the present report evaluates the biological response to two types of ENMs, zinc oxide (ZnO) and titanium dioxide (TiO₂), in three cell models that represent key exposure routes: dermal/implant, inhalation, and digestive. ZnO nanoparticles were chosen due to their potential to release Zn²⁺ ions and generate reactive oxygen species (ROS) (Wadekar et al., 2025; Belal et al., 2023). TiO₂ nanoparticles, which are widely used, show variable toxicity depending on their shape, size, and aggregation state (Chandoliya et al., 2024; Wolf et al., 2024).

The cell models include:

- NIH 3T3 mouse fibroblasts, with their spindle-shaped morphology ideal in pharmacological and oncogenic studies
- BEAS-2B bronchial epithelial cells, cultured at the air-liquid interface (ALI) to simulate occupational inhalation exposure (Gosselink et al., 2024).
- Caco-2 cells, which model intestinal absorption of nano-ingredients (Baranowska-Wójcik et al., 2024).

The main hypothesis is that the toxicological profile depends on both the ENM's chemistry and the cellular microenvironment. Before each experiment, nanoparticle size, shape, and stability in the relevant medium are characterized, using optical controls to verify dispersion. The experimental design uses realistic doses and wide ranges to determine the 50% inhibitory concentration, along with positive and negative controls. Exposures are submerged, except for the lung model, which also uses ALI (Gosselink et al., 2024). The variables analyzed include cytotoxicity (methylthiazol tetrazolium (MTT) and resazurin reduction as well as lactate dehydrogenase (LDH) assays), ROS, metal ion release, and nanoparticle internalization assessed by scanning electron microscopy with energy-dispersive X-ray spectroscopy (SEM/EDX), transmission electron microscopy and scanning transmission electron microscopy (TEM/STEM), micro X-ray fluorescence (μXRF), and micro X-ray absorption near-edge structure spectroscopy (μXANES).

Based on this, the report presents three specific case studies to assess different scenarios within the safe-by-design approach. These cases are:



- Case 1 (ZnO + NIH 3T3): Evaluates Zn²⁺ release and its impact on the dermal barrier, detecting oxidative stress and intracellular uptake at subcytotoxic levels.
- Case 2 (TiO₂ + BEAS-2B): Examines inhalation of nano-TiO₂, critical in industrial settings, using ALI to simulate real aerosol deposition compared to a submerged exposure.
- Case 3 (TiO₂ + Caco-2): Investigates effects of nano-TiO₂ in the gastrointestinal tract.

This report aims to demonstrate the usefulness of the NFFA workflow to assess nanomaterials and their interaction with different cell lines. It also seeks to generate improved protocols and educational material that can be shared with other European users working with similar ENMs.

2 Case 1: Dynamic evaluation of ZnO nanoparticles in NIH 3T3 fibroblasts

2.1 Context

This first case aimed to design, from a safe-by-design perspective, a platform to observe in real-time the interaction between uncoated ZnO nanoparticles and NIH 3T3 mouse fibroblasts under controlled dynamic conditions. The platform was developed through the integration of the following components:

- Polydimethylsiloxane (PDMS) substrates with microgrooves, fabricated via soft lithography, and inserted in an ibidi μ -slide I Luer 3D microfluidic chamber (Deliverable 14.2),
- An operando microscopy station (Deliverable 14.2),
- A liquid injection system integrated with the operando system, enabling controlled pulse injections of nanoparticles using a T-mixer validated for flow stability (Deliverable 14.3), and
- Complementary toxicity analyses, including cell viability (MTT) under static conditions and ROS generation (Milestone 5).

Nonlinear microscopy used in Deliverable 14.3 enabled real-time tracking of second harmonic generation (SHG) signals from ZnO nanoparticles at a validated safe concentration (1 μ g/mL). A continuous flow (15 μ L/min) of nutrient medium [DMEM-High Glucose (HG) medium without (w/o) fetal bovine serum (FBS) w/o penstrep (PS)] was used in the microfluidic system (Deliverable 14.2). By means of the syringe pump system, 200 μ L shots of 1 μ g/mL ZnO NPs were injected at a flow rate of 15 μ L/min into the flowing nutrient medium (Deliverable 14.3). The delay between each shot was set to 60 seconds and the duration of the NPs shots was 2 hours.

Viability tests confirmed that, after 24 hours of exposure, the 1 μ g/mL dose maintained high survival in NIH 3T3 fibroblasts (Deliverable 14.2, section In-vitro cytotoxicity study). In contrast, higher ZnO concentrations significantly reduced cell viability ($p < 0.01$, ANOVA), triggered intracellular ROS production from hour 6, and showed signs of nanoparticle degradation—findings detailed in Milestone 5 (In-vitro assays section).

The strength of this approach lies in three integrated components:

- PDMS substrates with 2D/2.5D geometries that support cell cultures under static and flow conditions (Deliverable 14.2, section Fabrication of the PDMS substrates),
- Operando microscopy station (Deliverable 14.2),



- Liquid injection system integrated with the operando system (Deliverable 14.3, section Integration of the injection system for liquids with the operando system), and
- Multimodal image acquisition using SHG, three-photon fluorescence (3PEF), and two-photon fluorescence (2PEF), also described in Deliverable 14.3.

Thanks to this combination, it was possible to observe in real-time the interaction of ZnO NPs with live cells under static and flow conditions, confirming short-term cell viability at the tested concentration.

2.2 Methodology

The methodology, described in detail in Deliverables 14.2 and 14.3 and Milestone 5, was structured into three main blocks: substrate design, injection system implementation, and exposure-analysis protocols. Higher concentrations (10–500 $\mu\text{g}/\text{mL}$) were only tested in static toxicity (MTT assay up to 500 $\mu\text{g}/\text{mL}$, Live Dead assay up to 100 $\mu\text{g}/\text{mL}$) and ROS generation assays (Deliverable 14.2 and Milestone 5). These were not subjected to continuous flow.

2.2.1 Fabrication of PDMS substrates via soft lithography (Deliverable 14.2)

The substrates were molded in PDMS using a 10:1 mixture of prepolymer and curing agent, a process that ensures optical transparency and biocompatibility. Flat (2D) and microgrooved(2.5D) substrates were fabricated, compatible with the μ -slide I Luer 3D chamber (ibidi).

The methodology, described in detail in Deliverables 14.2 and 14.3 and Milestone 5, was structured into three main blocks: substrate design, injection system implementation, and exposure-analysis protocols. Higher concentrations (10–100 $\mu\text{g}/\text{mL}$) were only tested in static toxicity and ROS generation assays (Deliverable 14.2 and Milestone 5). These were not subjected to continuous flow.

2.2.2 Integration of the injection system for liquids with the operando system (Deliverable 14.3)

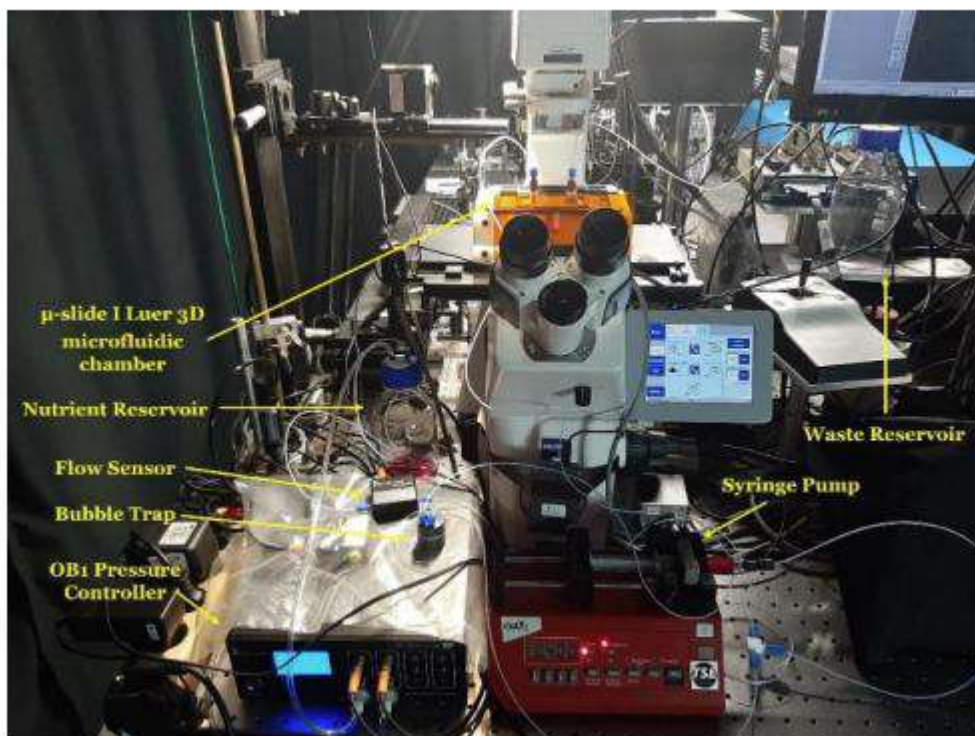


Figure 1: Illustration of the injection system for liquids with the operando system

Figure 1 (Deliverable 14.3, section Integration of the injection system for liquids with the operando system) shows the integrated system, which combines microfluidics, NLOM microscopy, and controlled NP injection. The setup includes:

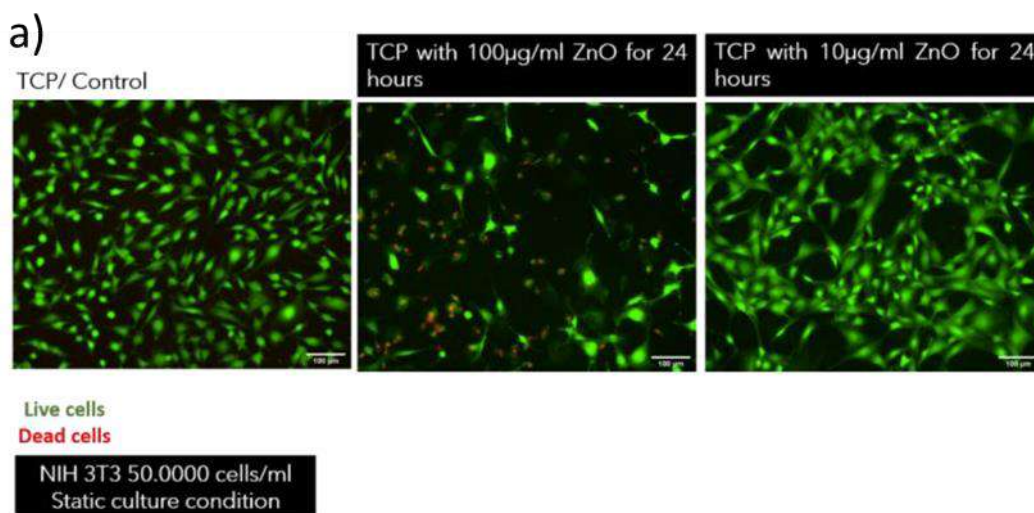
- An electronic syringe pump controlled by a custom LabView program,
- A T-mixer that merges the continuous flow of Dulbecco's Modified Eagle Medium (DMEM) with ZnO suspension pulses,
- A baseline flow rate of 15 $\mu\text{L}/\text{min}$ with 200 μL pulses injected every 60 seconds.

2.2.3 Exposure and analysis protocols (Milestone 5 + Deliverable 14.2)

The ZnO concentration selected for flow experiments (1 $\mu\text{g}/\text{mL}$) had been confirmed as non-toxic in static MTT assays (Deliverable 14.2). Concentrations ranging from 10–80 $\mu\text{g}/\text{mL}$ were reserved for studying reactive oxygen species (ROS) formation at 6, 24, and 48 hours, as detailed in Milestone 5. Image acquisition combined 3PEF (nuclei), 2PEF (membranes), and SHG (ZnO), following the Image acquisition protocol in Deliverable 14.3.

It is important to note that ROS assays were performed on static cultures; these data complement, but are not derived from the microfluidic flow experiments. To strengthen quantitative results, a Live/Dead assay (calcein/EthD-1) was performed. Fluorescence images in Figure 2 show that doses ≤ 10 $\mu\text{g}/\text{mL}$ maintain viability similar to controls. At 50 $\mu\text{g}/\text{mL}$, cell death increased significantly. Additionally, on microgrooved PDMS substrates, cells aligned along the grooves in contrast to flat substrates. This observation supports the documented biocompatibility (Deliverable 14.2).

The combination of PDMS substrates (Deliverable 14.2), microfluidics (Deliverables 14.2, 14.3), and toxicological analysis (Milestone 5) enables the evaluation of dynamic cell-NP interactions with greater physiological relevance than static assays.



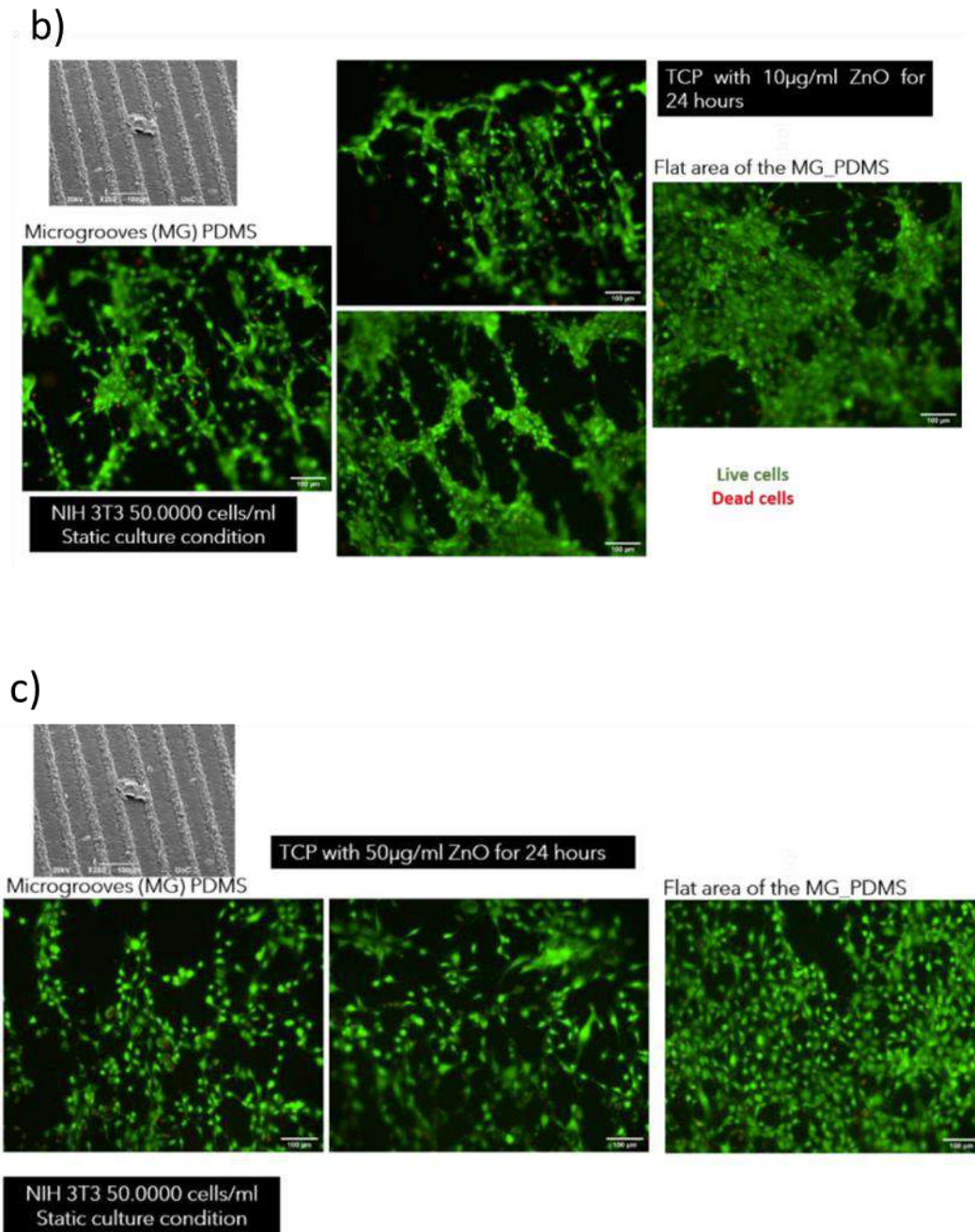


Figure 2: Live/Dead assay of mouse fibroblasts exposed to ZnO NPs. (a) After 24 hours of exposure to 100 and 10 µg/mL ZnO NPs; (b) after 24 hours of exposure to 10 µg/mL ZnO NPs; (c) after 24 hours of exposure to 50 µg/mL ZnO NPs.

2.3 Results

2.3.1 Cell viability

As described in Deliverable 14.2, NIH 3T3 fibroblasts adhered strongly and proliferated well on PDMS flat (2D) and microgrooved substrates (2.5D). It was also shown that ZnO nanoparticle (NP) concentrations $\leq 10 \mu\text{g/mL}$ maintained high cell viability after 24 hours. In contrast, concentrations $\geq 25 \mu\text{g/mL}$ caused cell toxicity (section Cytotoxicity of the ZnO NP solution).

A 30-minute ultrasonic pre-treatment was essential to ensure homogeneous NP dispersion and avoid imaging artifacts during second harmonic generation microscopy (section Observation of ZnO NPs with NLOM microscope).

2.3.2 Performance of the microfluidic injection system integrated with the operando system

As outlined in Deliverable 14.2, NIH 3T3 cells were cultured at a concentration of 700000 cells/mL on both flat and microgrooved PDMS substrates within the ibidi μ -slide I Luer 3D microfluidic chamber. The cells exhibited strong adhesion and proliferation on the PDMS substrates. After 24 hours of incubation, the samples were stained using Biotracker 555 Orange Cytoplasmic Membrane dye for the cell membrane and Hoechst dye for nuclei visualization. A continuous flow of DMEM-High Glucose (HG) medium without (w/o) fetal bovine serum (FBS) w/o penstrep (PS) was maintained at 15 μ L/min within the microfluidic system. Using a syringe pump system, 200 μ L injections of ZnO NPs at a concentration of 1 μ g/mL were delivered into the nutrient stream at a flow rate of 15 μ L/min. Each injection was spaced 60 seconds apart over a total duration of 2 hours (Deliverable 14.3). This specific concentration was selected based on findings in Deliverable 14.2, which demonstrated it to be non-toxic to NIH 3T3 cells. Using the NLOM microscope, nuclei, cell membranes, and ZnO NPs were observed within the μ -slide I Luer 3D microfluidic chamber. Furthermore, under the 1 μ g/mL ZnO NPs shots, NIH 3T3 cells remained alive inside μ -slide I Luer 3D microfluidic chamber further supporting the biocompatibility of this concentration as previously reported in Deliverable 14.2 (Figures 3, 4).

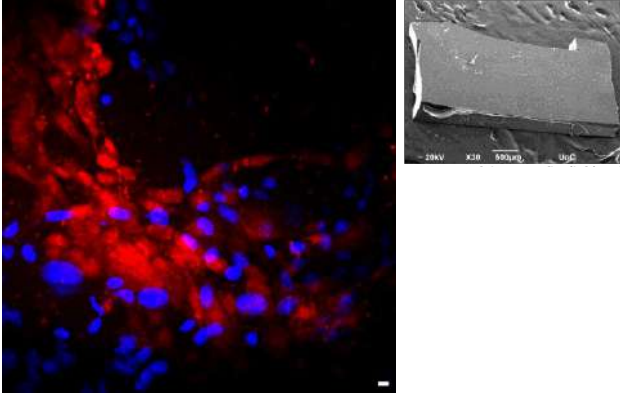
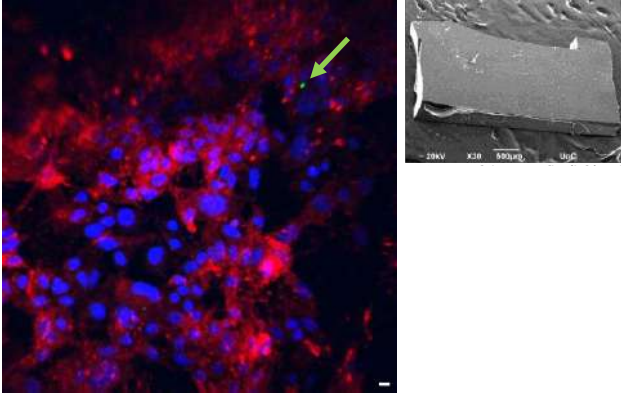
Before 1 μ g/mL ZnO NPs shots	After 1 μ g/mL ZnO NPs shots
	
<p>Hoechst (nuclei): 3PEF signal</p> <p>Biotracker 555 Orange Cytoplasmic Membrane dye: 2PEF signal</p>	<p>Hoechst (nuclei): 3PEF signal</p> <p>Biotracker 555 Orange Cytoplasmic Membrane dye: 2PEF signal</p> <p>ZnO NPs: SHG signal</p>
<p>PDMS flat substrate</p>	

Figure 3: Observation of live NIH 3T3 cells cultured on PDMS flat substrate inside ibidi μ -slide I Luer 3D microfluidic chamber with the NLOM microscope before and after the ZnO NPs shots. Scale bar: 10 μ m. The inset SEM images depict the PDMS flat substrate.

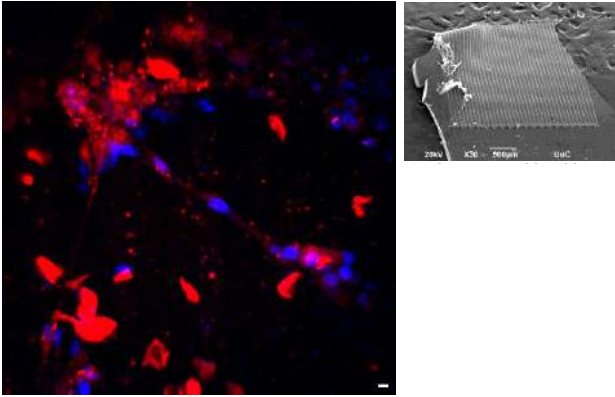
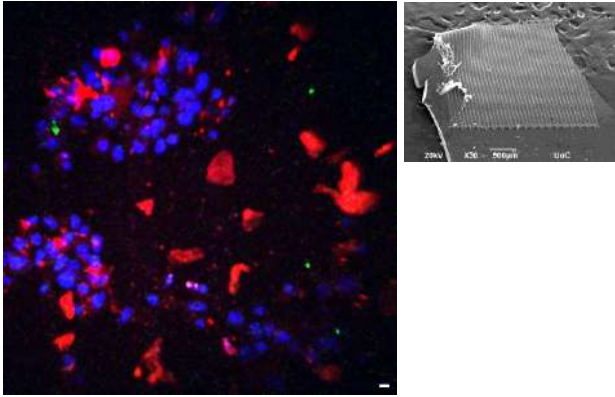
Before 1 μ g/mL ZnO NPs shots	After 1 μ g/mL ZnO NPs shots
	
<p>Hoechst (nuclei): 3PEF signal</p> <p>Biotracker 555 Orange Cytoplasmic Membrane dye: 2PEF signal</p>	<p>Hoechst (nuclei): 3PEF signal</p> <p>Biotracker 555 Orange Cytoplasmic Membrane dye: 2PEF signal</p> <p>ZnO NPs: SHG signal</p>
<p>PDMS microgrooved substrate</p>	

Figure 4: Observation of live NIH 3T3 cells cultured on PDMS microgrooved substrate inside ibidi μ -slide I Luer 3D microfluidic chamber with the NLOM microscope before and after the ZnO NPs shots. Scale bar: 10 μ m. The inset SEM images depict the PDMS microgrooved substrate.

2.3.3 Toxicological analysis and intracellular location of NPs

Cell viability showed a clear dose dependence. At 20 μ g/mL, a significant reduction was observed after 48 hours ($p < 0.01$, ANOVA), while concentrations ≥ 50 μ g/mL triggered increased production of reactive oxygen species (ROS) starting at 6 hours, preceding the loss of viability (Milestone 5, section In-vitro assays).

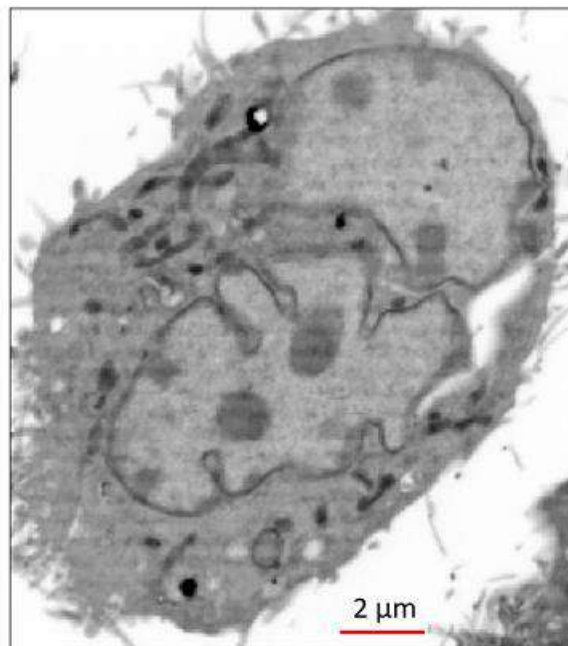


Figure 5: Synchrotron XRF imaging analyses of NIH 3T3 cells exposed to 10 μg/mL ZnO NPs for 6h performed at ESRF beamline ID16B. Os-L XRF image (pixel size: 60 nm)

Using electron microscopy (TEM/STEM), morphological changes were observed in NPs internalized within endosomes after 48 hours, indicating intracellular degradation (Milestone 5, section TEM analysis). Synchrotron-based analyses (XRF/XANES) revealed limitations due to signal overlap between osmium (Os) and zinc (Zn) in samples analyzed after 6 hours at beamline ID16B (ESRF) (Figure 5). However, preliminary XANES spectra from beamline ID21 suggested chemical modifications of the internalized ZnO (Milestone 5, section Synchrotron analysis) (Figure 6).

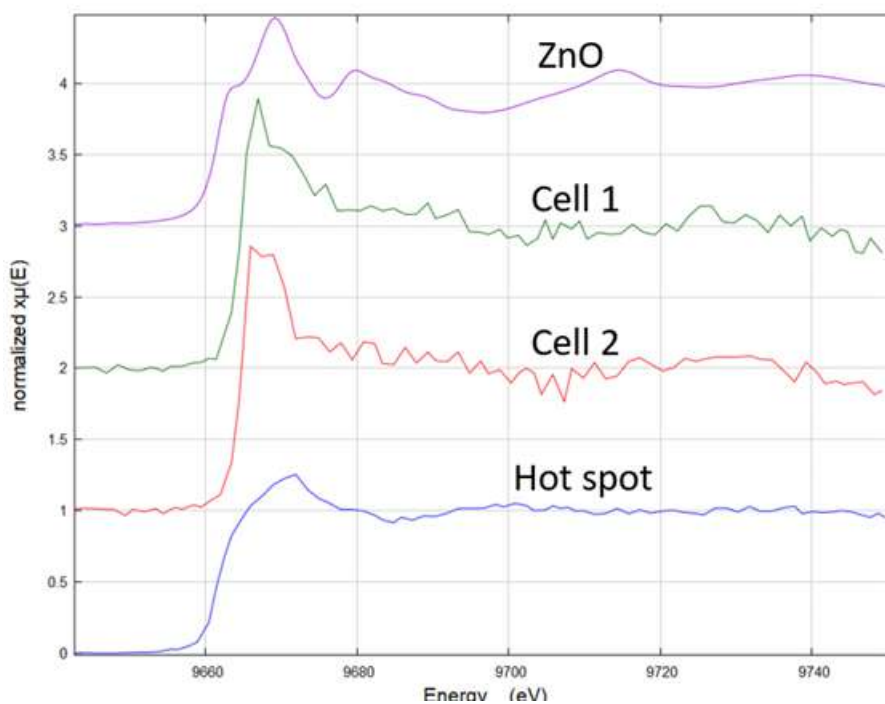


Figure 6: Synchrotron XANES analyses of NIH 3T3 cells exposed to 10 μg/mL ZnO NPs for 48h performed at ESRF beamline ID21.

2.3.4 Global integration and limitations

The system demonstrated robustness in three key aspects: Biocompatibility on PDMS substrates (Deliverable 14.2), Precision in controlled NP delivery via microfluidics (Deliverable 14.3), and Correlation between reduced viability, ROS generation, and intracellular NP degradation (Milestone 5). However, certain limitations were identified. A major issue was the tendency of ZnO NPs to aggregate, especially at concentrations $\geq 50 \mu\text{g/mL}$. This required a prior ultrasonic treatment to ensure proper dispersion and avoid imaging artifacts (Deliverable 14.2).

2.4 Conclusions

A microfluidic platform (liquid injection system integrated with the operando system) was successfully developed, integrating controlled NP injection, NLOM microscopy, and cell culture under flow conditions, as proposed in Deliverable 14.3. The results helped define key safety parameters and evaluate the technical feasibility of the proposed workflow. A ZnO NP concentration of $1 \mu\text{g/mL}$ was found to maintain high cell viability in NIH 3T3 fibroblasts after 24 hours. This was confirmed by MTT assays and supported by oxidative stress and long-term toxicity studies presented in Milestone 5.

Equally, concentrations $\geq 50 \mu\text{g/mL}$ triggered ROS production from hour 6 and led to a strong decrease in viability by 48 hours, linked to intracellular degradation of the nanoparticles observed through TEM/STEM.

From a technical perspective, NLOM microscopy allowed simultaneous detection of ZnO NP second harmonic signals, 3PEF from cell nuclei, and 2PEF from cell membranes. This enabled real-time tracking of cell-NP interactions, as shown in Deliverable 14.3.

A notable limitation was NP aggregation, which required a mandatory ultrasonic step for homogeneous dispersion, also documented in Deliverable 14.2.

Overall, the platform provides a solid foundation for assessing nanomaterial safety under dynamic conditions and for applying safe-by-design principles from the early stages of development. The system not only met the initial objectives but also serves as a reproducible model for future nanotoxicology studies.

3 Case 2: Aerosol exposure to TiO_2 NPs in BEAS-2B bronchial cells

3.1 Context

Case 2 continues the safe-by-design approach, now applying it to the characterization of TiO_2 nanoparticles (TiO_2 -NPs) in a pulmonary exposure model using human bronchial epithelial cells (BEAS-2B). The main objective is to perform correlative measurements in the same cellular area by combining SEM/STEM, μXRF , and μXANES .



This integration allows the collection of complementary information about the chemical and biological environment surrounding TiO₂-NPs, improving result accuracy by directly comparing electron microscopy data with synchrotron-based spectroscopic analyses.

The experimental workflow followed five stages, previously reported in Milestone 29:

- The NACIVT aerosol exposure chamber (developed by Lund University, Sweden) was used to ensure uniform TiO₂-NP distribution over the cells, simulating physiological conditions (Milestone 20).
- BEAS-2B cells were exposed to TiO₂-NPs for various durations in the NACIVT chamber, ensuring reproducible contact with the cultures.
- After exposure, samples were prepared and analyzed by transmission electron microscopy (TEM) at the Joint Research Centre (JRC, Ispra).
- More detailed imaging was conducted using SEM/STEM at the AREA Science Park/CNR-IOM (Trieste, Italy) to locate specific cells of interest.
- Finally, μ XRF and μ XANES experiments were conducted at the ESRF (Grenoble, France).

In addition to these five steps covered in Milestone 29, this report presents three additional developments that were not previously consolidated:

- Cytotoxicity evaluation following aerosol exposure (Lund University) and liquid phase (submerged, SUB) exposure (INL, Portugal),
- Precise localization of target cells via SEM/STEM,
- Acquisition of μ XRF maps from the same cells previously analyzed by SEM/STEM.

With these new results, the remaining objectives from Milestone 29 are fulfilled, achieving full integration of correlative SEM/STEM and μ XRF studies. This provides a more detailed view of the behavior of TiO₂-NPs in the airway exposure model.

3.2 Methodology

3.2.1 Aerosol exposure of BEAS-2B cells to TiO₂ NPs (Milestone 29)

The cytotoxicity of anatase TiO₂ nanoparticles (TiO₂-NM102-JRCNM10202a) was evaluated on BEAS-2B human bronchial epithelial cells. Aerosols were generated using a nebulizer connected to the NACIVT exposure chamber developed during Milestone 5. The experimental setup included two exposure durations (1h and 3h), two post-exposure fixation times (24h and 48h), and control samples treated only with water. Cytotoxicity was assessed using the lactate dehydrogenase (LDH) assay.

3.2.2 Sample preparation

After exposure, cells were collected, dehydrated, and embedded in epoxy resin before being sectioned into ultrathin slices. Samples were divided into two batches: one for SEM/STEM analysis (Area Science Park, Trieste), and the other for μ XRF/ μ XANES experiments (ESRF beamline ID21, Grenoble). Shipment to ESRF required an import permit for human biological material (IE-2024-4349, 18 December 2024). In parallel, the INL laboratory conducted liquid-phase exposure assays using the same BEAS-2B cell line and identical TiO₂ material and nanoparticle concentrations, to compare results with the aerosol exposure model.



3.3 Results

3.3.1 Preliminary results before correlative analysis (Milestone 29)

Initial analyses from Milestone 29 focused on TiO₂-NP characterization and their interaction with cells. The nanoparticles showed an aggregated morphology, forming clusters of ~500 nm composed of individual particles with an average diameter of 21.9 ± 12.2 nm (Milestone 29, section 3.1). Cellular internalization of TiO₂-NPs was confirmed only in the condition 3h_TiO₂_24h, via TEM. In other tested conditions, NPs were not detected inside the studied cells (Milestone 29, section 3.3). SEM/STEM imaging enabled precise localization of cells that had internalized TiO₂-NPs, facilitating subsequent correlative analysis. μ XRF and μ XANES studies detected titanium signals on the cell surface for the 3h_TiO₂_24h condition. Furthermore, μ XANES confirmed that the NPs retained their anatase phase (see Figure 7). In contrast, the 3h_TiO₂_48h condition showed fewer titanium signals, and a minor presence of the rutile phase was detected, likely due to contamination (section 3.5).

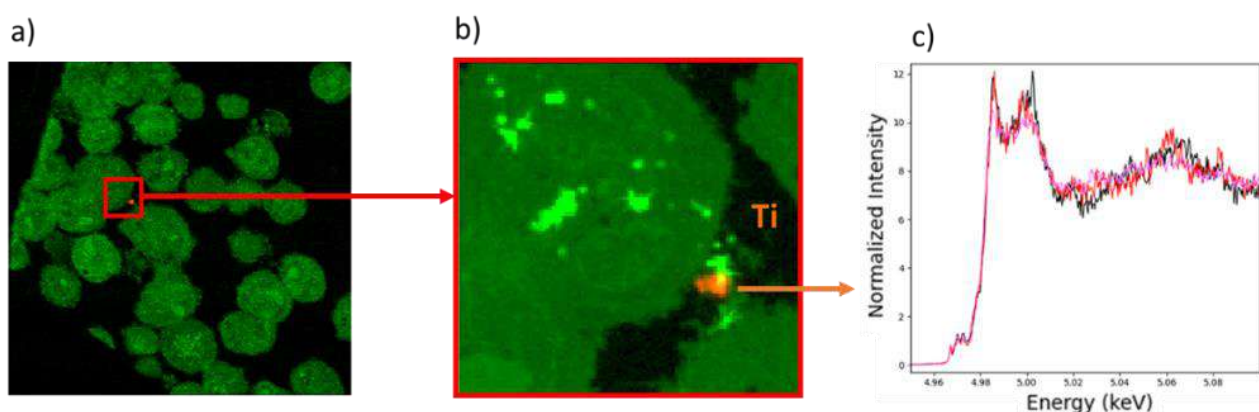


Figure 7. μ XRF maps and μ XANES for sample 3h_TiO₂_24h (a) Os (green) and Ti (red) distribution across an $80 \times 80 \mu\text{m}^2$ area. (b) Zoom-in of the region of interest ($16 \times 16 \mu\text{m}^2$). (c) Ti K-edge XANES spectra acquired in the Ti-enriched region.

These results demonstrated the capacity of the applied methodology to characterize both the properties of TiO₂-NPs and their cellular interactions under different experimental conditions.

3.3.2 Correlative SEM/STEM and μ XRF analysis in sample 3h_TiO₂_24h

The 3h_TiO₂_24h sample, previously identified in section 3.1 as the most promising for detecting TiO₂-NP internalization, was analyzed in detail in this section. A complete scan of the sample was performed using SEM/STEM to locate areas of interest. During this process, a particularly promising region was identified (Figure 8a), clearly showing several BEAS-2B cells (purple box). This area was selected as the region of interest for follow-up analysis. In the upper-right corner of the image (Figure 8a), a shadow caused by the sample holder is visible, though it does not interfere with the visualization of the cells.

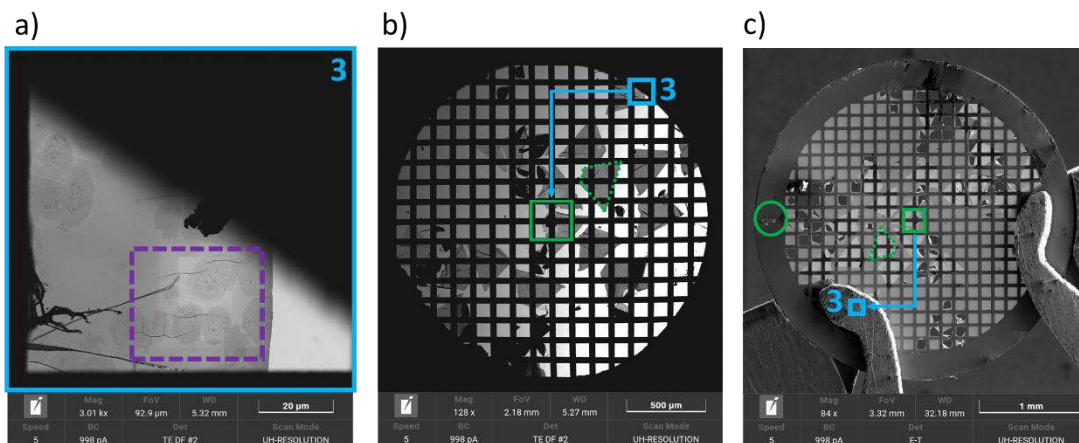


Figure 8. Multiscale SEM/STEM localization of the region of interest in the sample 3h_TiO₂_24h.

(a) High-magnification SEM/STEM image showing BEAS-2B cells in the purple box. (b) Lower magnification image identifying window 3 (cyan), grid center (green square), and trapezoid marker (green dashed line). (c) Global SEM/STEM image after flipping the grid, confirming window "3" and reference marker 1 (green circle).

A lower-magnification view (Figure 8b) revealed a broader area of the same grid. In this image, a cyan box marks the specific "window 3", where the cells of interest are located. A green square indicates the center of the grid, and a green dotted trapezoid outlines one of the resin sections. These visual elements confirm the exact position of window 3 within the grid. Finally, after inverting the grid, a global image was taken (Figure 8c), again showing window "3" and a green-circled number "1", both serving as key references for locating the cells during the upcoming μ XRF analysis.

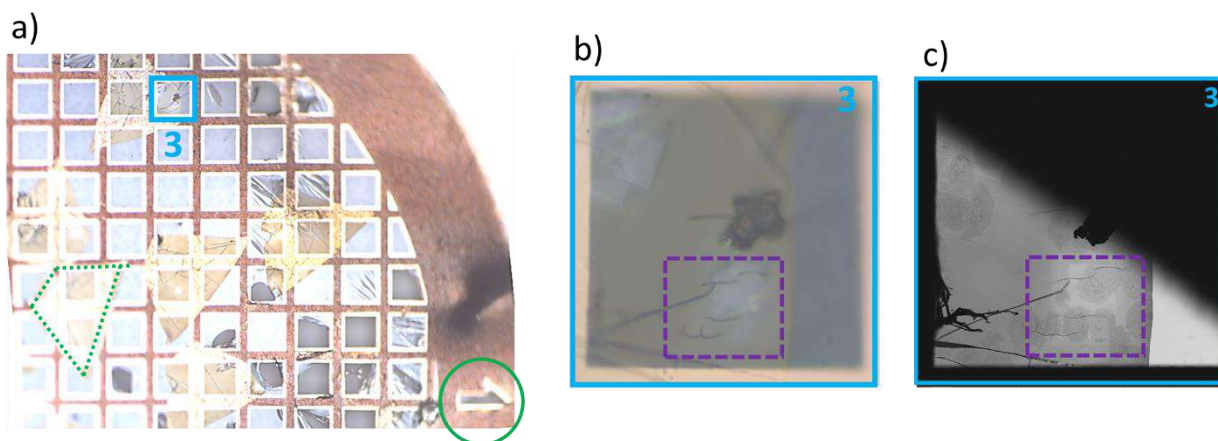


Figure 9. Optical Confirmation and Delimitation of the μ XRF Area in Window 3 at ID21 (a) Optical overview of the entire grid showing all known markers and window 3. (b) Zoom-in of window 3, with recognizable patterns and the purple measurement area. (c) SEM/STEM image from Trieste corresponding exactly to the same region as (b).

Once receiving the sample at ID21-ESRF, an optical image of the full grid was first acquired (Figure 9a). The same cyan markers, green circle, and dotted trapezoid were identified, helping confirm the precise location of window 3. A zoomed optical view (Figure 9b) shows the exact same patterns previously identified via SEM/STEM, allowing a precise definition of the region of interest (purple box) for μ XRF mapping. The original SEM/STEM image (Figure 9c) confirms a good spatial match with the optical view, verifying that both images focus on the same region.

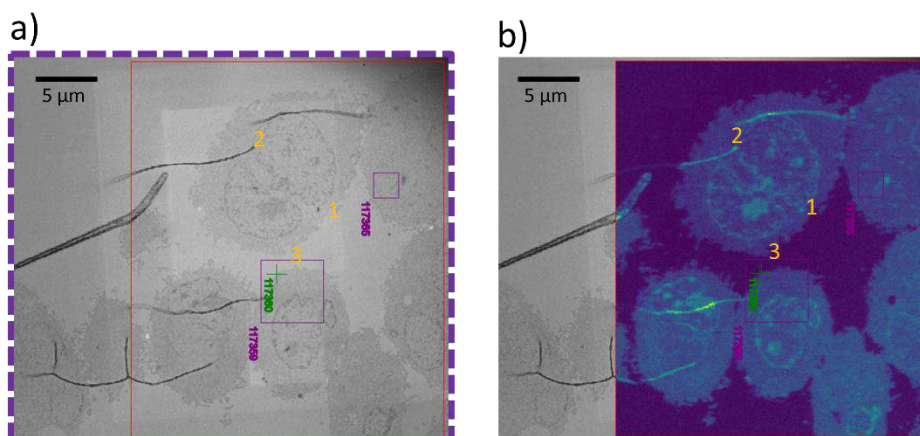


Figure 10. Coordinate Transformation and Registration Between SEM/STEM and μ XRF (a) SEM/STEM image with fiducial points 1–3 marked in orange. (b) Chlorine μ XRF map ($25 \times 30 \mu\text{m}^2$) showing accurate alignment with (a); the gray band indicates a non-scanned area.

Next, a μ XRF map was acquired within the area defined by the purple box, covering approximately $25 \times 30 \mu\text{m}$ (Figure 10b). This map, based on chlorine emission (an element abundant in cells), revealed clearly recognizable cell structures. Three fiducial points (orange, numbered 1–3) were selected from these structures and were then matched with the same features in the SEM/STEM image (Figure 10a). Using these reference points, the Daiquiri software calculated a precise coordinate transformation between the SEM/STEM image and the NanoSXM μ XRF scanner at ID21. The success of this transformation is demonstrated by the excellent alignment of fiducial points and structural features between both imaging modalities (Figure 8a and 8b). Although a titanium signal was specifically searched for in the μ XRF map, it did not exceed the background noise level. As a result, μ XANES spectroscopy for Ti was not performed. This outcome is consistent with earlier observations in section 3.1, which reported that detectable internalization of TiO_2 nanoparticles in BEAS-2B cells is infrequent. Despite the lack of μ XANES data, the experiment successfully confirmed a precise spatial correspondence between SEM/STEM imaging and μ XRF mapping, a critical step toward reliable correlative analysis of nanomaterial-cell interactions.

3.3.3 Validation under submerged exposure: replication of the experiment by INL

The Nanosafety Research Group at INL took over the task to replicate the experiments performed in Lund University but considering a submerged cellular exposure instead of an ALI one. For that, all experimental parameters set up in Lund were mimicked, including cell line and culture conditions, material under analysis (i.e., TiO_2 -NPs), NP concentrations and time of exposure, as well as endpoints, as summarized in Table 1.

Table 1 Experimental setup comparison: ALI vs. submerged exposure models

Partner	Uni Lund	INL
Cell line	BEAS-2B	
Cell culture medium	RPMI1640 w/ 10% FBS, 1% PenStrep	
Cell density	50000 cells/insert	



Insert type/brand	24-well plate, polyester membrane, 0.33 cm ² growth area, pore size 0.4 μm (VWR)	
Material	TiO ₂ -NPs, shared between the groups	
Concentrations	10 and 30 μg/cm ²	
NP suspension prep	0.5 mg/mL TiO ₂ -NPs in ultrapure water, 30min in ultrasound bath	Same as Lund (NEP) <i>versus</i> Nanogenotox
Type of exposure	Aerosol @ALI	Submerged
Time of exposure	1 and 3h – endpoint measured at 24 and 48h	24 and 48h
Endpoints	<ul style="list-style-type: none"> - Resazurin-based metabolic activity - LDH assay 	

Before the experiments with cells, the NP suspensions were characterized using dynamic light scattering (DLS) and nanoparticle tracking analysis (NTA) to understand their size distribution according to the selected preparation protocol. As shown in Figure 11, the results indicate that both dispersion protocols yield similar sized populations of around 200nm hydrodynamic size, though the Nanogenotox protocol results in a smaller polydispersity index.

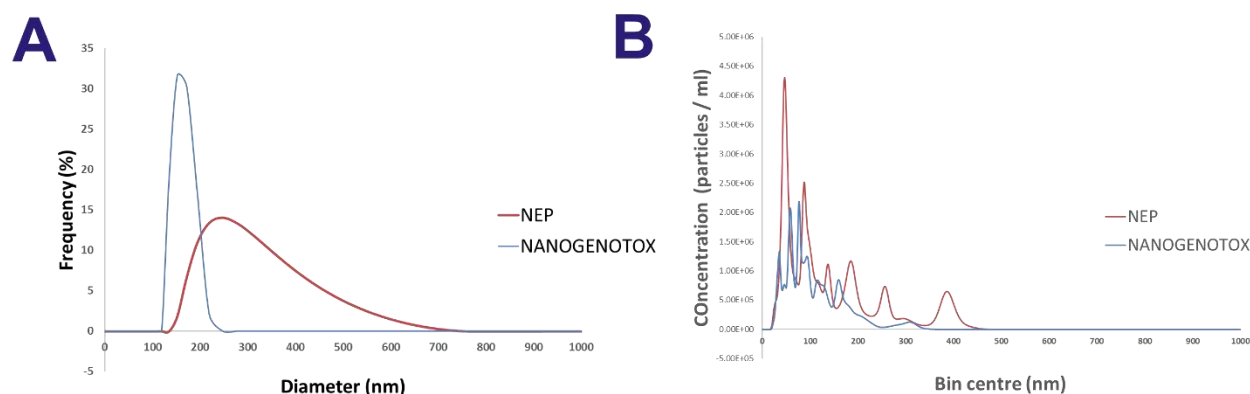


Figure 11 – Graphical representation of diameter (nm) vs frequency (%) obtained from (A) DLS analysis of TiO₂-NP stock suspension prepared according to the NEP protocol vs NANOGENOTOX protocol and (B) summary graph of bin centre (nm) vs concentration (particle/ml) from NTA results of exposure TiO₂-NPs suspension at 30 μg/cm² prepared according to NEP protocol vs Nanogenotox. DLS measurements performed on a SZ-100Z Particle Analyzer (Horiba Scientific) at room temperature, scattering angle 90°, measurement duration 60 seconds. NTA measurements performed on a Malvern Panalytical Nanosight NS300 at room temperature, 5 videos duration of 60 seconds each.

A pilot experiment was run to test growing concentrations of TiO₂-NPs on a 24h submerged exposure of BEAS-2B cells. Cellular metabolic activity, measured as the ability of cells to reduce resazurin to highly fluorescent compound, resorufin, was used as surrogate for cellular viability. We observed an apparent decline in cell viability with increasing NPs concentration, with a maximum effect at 60 μg/cm² (Figure 12A). This experiment allowed us to confirm that the concentrations selected for the ALI exposure, namely 10 and 30 μg/cm², are suitable for the submerged exposure, as well.

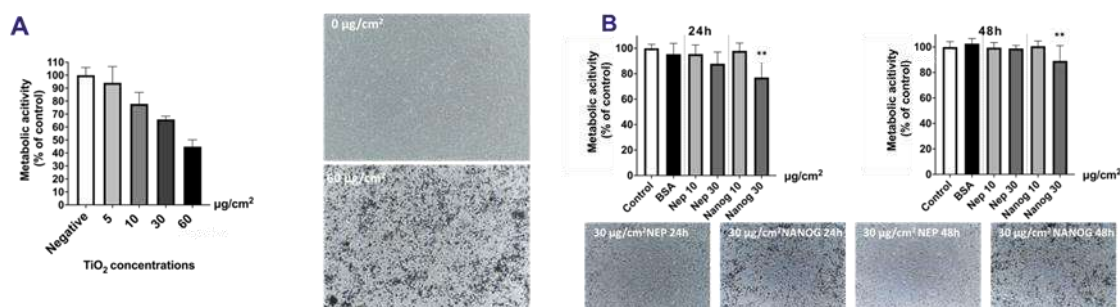


Figure 12. Metabolic activity (expressed as % of untreated control) as evaluated through resazurin reduction assay and the corresponding images in the pilot study (A) and after incubation for 24h and 48h of BEAS-2B cells with selected concentrations of TiO₂-NPs (B). The results are presented as mean ± standard deviation (SD) from one (pilot test A) or three independent experiments (B) with at least two replicates each. Statistical comparisons were made using one-way ANOVA (**p ≤ 0.01 vs control, GraphPad Prism Software v9). Images acquired with a NIKON ECLIPSE TS2-FL inverted routine microscope (100x magnification).

The effects of TiO₂ NP on cell viability after a 24 and a 48h exposure of BEAS-2B cells under submerged conditions are summarized in Figure 12B. The tested TiO₂-NPs induced a significant decrease in cell viability at both time-points, for the highest tested concentration when dispersing the NPs following the Nanogenotox protocol.

To confirm these results, a second endpoint, LDH activity, was measured using the cell culture medium collected from the basolateral compartment after 24 and 48h of exposure. LDH is a cytoplasmic enzyme that is released to the extracellular medium upon disruption of the cellular membrane, usually a sign of cell death. As shown in Figure 13, the results show no statistically significant changes in the LDH release for the tested conditions compared to the negative control (cell culture media of the untreated cells). We highlight, however, that these results are not yet final as they are still not corrected for the total LDH levels (full kill – currently ongoing), which may change the overall results.

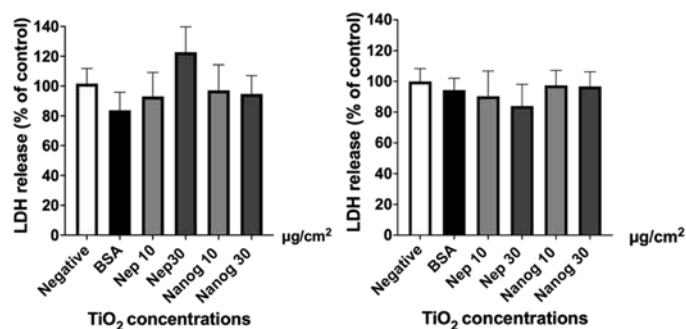


Figure 13 – Extracellular LDH released by BEAS-2B cells after 24 and 48h incubation with selected TiO₂-NP concentrations. LDH was quantified in the basolateral media. Results are presented as percentage of extracellular LDH relative to the negative control. The results are presented as mean ± standard deviation (SD) from three independent experiments with minimum two replicates each. Statistical comparisons were made in GraphPad Software using one-way ANOVA.

After the cytotoxicity assays, a correlative microscopy approach similar as in section 3.3.2 for TiO₂ in bronchial cells will be followed. The cell culture is in progress and results will be detailed in the final report of year 2025 for WP14.

3.4 Conclusions

The NACIVT chamber at LUND was successfully used to expose BEAS-2B cells to TiO₂ NPs simulating airway exposure. SEM imaging of cells incubated with TiO₂ NPs was performed using different SEM modes, highlighting regions compatible with the presence of TiO₂ NPs uptaken by the cells. Using a correlative approach STEM and Synchrotron X-ray imaging a low level of internalization of TiO₂ NPs was evidenced. Under submerged exposure, and using the dispersion protocol used at Lund University, TiO₂-NPs did not induce significant effects to BEAS-2B cells with regards to cellular metabolism and extracellular LDH levels. However, when using the Nanogenotox dispersion protocol, a significant decrease in cellular metabolic activity was observed for the highest tested concentration, possibly indicating cell viability impairment. This effect was confirmed with optical microscopy. The less polydisperse and potentially more stable nanoparticle population obtained with the Nanogenotox protocol may justify the observed results.

4 Case 3: Exposure to TiO₂ Nps in Caco-2 colon cells

In a preliminary test, Caco-2 cells were exposed to the NPs prepared following the Lund protocol and cell viability was inquired after 24h of exposure in submerged conditions. The results indicate that the Caco-2 cell viability was not affected by any of the tested concentrations Figure 12. In parallel, we have seeded cells that are currently under differentiation for 21 days to be, then,



exposed to the different NP concentrations. Cellular differentiation will be followed by measuring the transepithelial electrical resistance (TEER) and visualizing the formation of villi in the epithelial tissue.

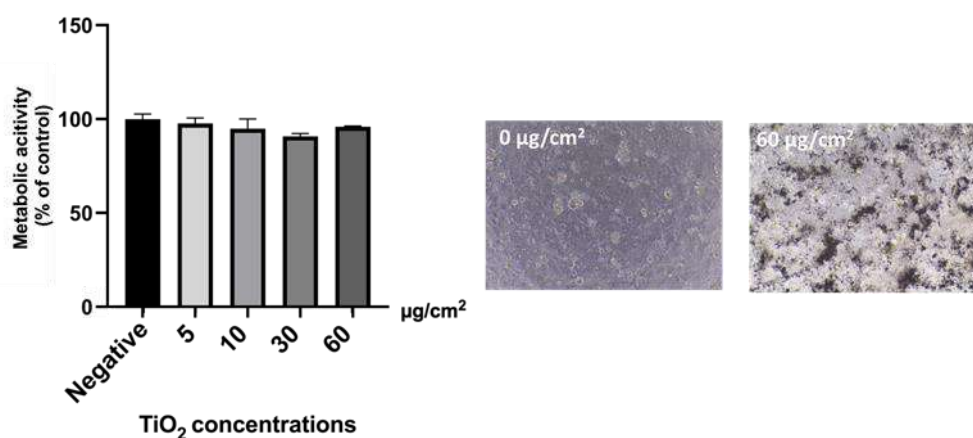


Figure 14 – Metabolic activity (expressed as % of untreated control) as evaluated through resazurin reduction assay and the corresponding images in the pilot study of 24h incubation for Caco-2 cells with growing concentrations of TiO₂-NPs. The results are presented as mean ± standard deviation (SD) from at least two replicates per condition. Images acquired with a NIKON ECLIPSE TS2-FL inverted routine microscope (100x magnification).

After the cytotoxicity assays, a correlative microscopy approach (similar as in section 3.3.2) for TiO₂ in the colon cells will be followed. The cell culture is in progress and results will be detailed in the final report of year 2025 for WP14.

5 OUTCOMES

- The developed microfluidic platform enabled the evaluation of dynamic interactions between NPs and living cells.
- ZnO nanoparticles exhibited high cell viability at low concentrations (≤ 10 µg/mL), whereas higher doses (≥ 50 µg/mL) induced early oxidative stress and significantly decreased cell viability.
- Effective dispersion of the ZnO nanoparticles required prior ultrasonic treatment to prevent aggregation and image interference.
- NIH 3T3 cells showed good attachment and growth on the microstructured PDMS substrates.
- The NLOM allowed simultaneous real-time monitoring of NPs and cells.
- The developed microfluidic platform embedded with the NLOM (operando microscopy platform) enabled the real-time monitoring and evaluation of dynamic interactions between NPs and living cells. ZnO nanoparticles exhibited high cell viability at low concentrations (≤ 10 µg/mL), whereas higher doses (≥ 50 µg/mL) induced early oxidative stress and significantly decreased cell viability.

- In the lung model (BEAS-2B), SEM/STEM and μ XRF images were accurately correlated, although internalization of TiO₂ nanoparticles was rare.
- Overall, the proposed methodology validates the safe-by-design approach and offers reproducible protocols for future nanotoxicology studies.

6 References

- Trump, B.D., Poinssatte-Jones, K., & Linkov, I. (2024). Safety-by-design and engineered nanomaterials: the need to move from theory to practice. *Environment Systems & Decisions*, 44, 177-188. <https://doi.org/10.1007/s10669-023-09927-w>
- De Angelis, D., Dalla Torre, G., Zonno, M., et al. (2025). FDO-Based FAIR-by-Design upgrade of an interdisciplinary research infrastructure for nanoscience. *Open Conference Proceedings*, 5. <https://doi.org/10.52825/ocp.v5i.1201>
- Chandoliya, R., Thakur, P., Yamgar, R., et al. (2024). Titanium dioxide nanoparticle: A comprehensive review on synthesis, applications and toxicity. *Plants*, 13(21), 2964. <https://doi.org/10.3390/plants13212964>
- Wadekar, S.R., Hate, M.S., & Chaughule, R.S. (2025). Biosynthesis of zinc oxide nanoparticles and their cytotoxicity study on fibroblast cell line using MTT assay. *Oriental Journal of Chemistry*, 41(2). <https://doi.org/10.13005/ojc/410209>
- Belal, R., & Gad, A. (2023). Zinc oxide nanoparticles induce oxidative stress, genotoxicity, and apoptosis in the hemocytes of *Bombyx mori* larvae. *Scientific Reports*, 13, 3520. <https://doi.org/10.1038/s41598-023-30444-y>
- Wolf, S., Kuehnert, T., Creutzenberg, O., et al. (2024). Systematic review of mechanistic evidence for TiO₂ nanoparticle-induced lung carcinogenicity. *Nanotoxicology*, 18(5), 437-463. <https://doi.org/10.1080/17435390.2024.2384408>
- Gosselink, I.F., Guimarães, E., Bos, S., et al. (2024). Assessing toxicity of amorphous nanoplastics in airway- and lung epithelial cells using air-liquid interface models. *Chemosphere*, 368, 143702. <https://doi.org/10.1016/j.chemosphere.2024.143702>
- Baranowska-Wójcik, E., Matwijczuk, A., Szusarczyk, K., et al. (2024). Effect of food additive E171 and titanium dioxide nanoparticles (TiO₂-NPs) on Caco-2 colon cancer cells. *Applied Sciences*, 14(20), 9387. <https://doi.org/10.3390/app14209387>

